

Design, Model, and Manufacture an Internal Combustion Engine

This report represents the work of one or more WPI undergraduate students submitted to the faculty as evidence of completion of a degree requirement.

WPI routinely publishes these reports on the web without editorial or peer review.

by

Qianchen Zeng

April, 2023

Project Advisor:

Alireza Ebadi

Abstract

The aim of this project is to investigate the use of PLA material and 3D printing technology to create a model of the Toyota 4A internal combustion engine. The 3D printed model of the engine has potential applications in education, testing, development, and prototyping of new engine designs.

The engine model was created with 3D modeling software, and printed with an FDM printer. Theoretical kinematic and dynamic analyses are performed, and results are compared with simulations. Furthermore, the tensile properties of the printing material are tested with different printing angles and infill percentages for more accurate analyses.

Contents

1	Introduction	1
2	Modeling Background	3
2.1	software and Hardware	3
2.2	Engine	3
3	Tensile Testing	5
3.1	Dogbond Specimen	6
3.2	Result from Instron Tensile Machine Experimentation	7
4	Kinematic Analysis	12
4.1	Diagram	13
4.2	Hand Calculation	14
4.3	Solidwork Simulation	16
4.3.1	Piston Displacement	16
4.3.2	Linear Velocity of Piston	17
4.3.3	Angular Velocity of Connecting Rod	17
4.3.4	Angular Acceleration	18
5	Dynamic Analysis	19
5.1	Diagram	19
5.2	Hand Calculation	20
5.3	Solidworks Simulation	21
6	Conclusion	22

7 Impact	23
7.1 Safety	23
7.2 Environment	23
7.3 Education	24
7.4 Economic	24
Appendices	25
A CAD Drawing	26

List of Figures

3.1	Standard dogbone specimens dimensions.	6
3.2	Tensile testing by using Instron machine.	7
3.3	Tensile testing result of dogbone specimen printed in 0 degree and 50% infill rate.	8
3.4	Tensile testing result of dogbone specimen printed in 0 degree and 100% infill rate.	9
3.5	Tensile testing result of dogbone specimen printed in 45 degree and 100% infill rate.	9
3.6	Tensile testing result of dogbone specimen printed in 90 degree and 100% infill rate.	10
3.7	Table 3.3: Results from the tensile testing.	10
4.1	Diagram that represents the piston (blue), connecting rod (red), and crankshaft(yellow).	13
4.2	Piston displacement graph generated from Solidworks motion analysis.	16
4.3	Motion analysis of linear velocity of piston using Solidworks	17
4.4	Motion analysis of angular velocity of connecting rod using Solidworks.	17
4.5	The hand calculated angular acceleration of the connecting rod graphed using Desmos.	18
5.1	Free body diagram of the crankshaft system.	19
5.2	Reaction force between piston and cylinder body generated by matlab.	21

Chapter 1

Introduction

The internal combustion engine (ICE) is a mechanical device that generates power by burning fuel within a cylinder. It typically uses gasoline or diesel, and operates on the principle of converting chemical energy into mechanical energy. ICEs are most commonly found in automobiles. The engine's main components are the cylinder, piston, connecting rod, and crankshaft. These components will make up into a cranks slider system. From another MQP project about cranks slider, we could easily get to know the engine motion better[1].

3D printing an ICE can be very useful in education. A 3D printed ICE model can serve as an effective visual aid, helping students better understand the engine's components and functionality, thereby create a deeper appreciation for mechanical engineering and automotive technology. It could also be very challenging. ICEs require precise manufacturing and tight tolerances to ensure proper fit and movement of components. Achieving the necessary accuracy with 3D printing can be challenging. The material I will be using is PLA (polylactic acid). PLA can be prone to warping or shrinkage during cooling, which might affect the accuracy and tolerances of the printed ICE model. Therefore, multiple printings will be needed to achieve the desired tolerance. Furthermore, PLA parts are printed layer-by-layer, which can result in weaker connection between layers. This could cause the model's components to delaminate or fail under stress, particularly if the model is subjected to any operational forces or pressures. In this case, I will also be conducting tensile

test on the PLA material and find the optimal printing setting for PLA.

Tensile testing is crucial in evaluating the properties of PLA 3D printed parts, as it helps determine their suitability for various applications. Tensile testing provides valuable information on the strength, elongation, and modulus of elasticity of 3D printed PLA parts, enabling users to assess the material's performance under tension and make informed decisions about its applicability. Tensile testing can also help identify the impact of printing parameters, such as print speed, layer height, and infill rate, on the properties of PLA parts. By analyzing the results, users can optimize these parameters to achieve desired strength and durability.

Chapter 2

Modeling Background

In this chapter, I will be listing the software and hardware used during this project and the information on the engine that I will be modeling.

2.1 software and Hardware

3D modeling software: Solidworks, Creo

3D printer: Creality Ender-3 Max Neo (FDM Printer)

Printing Material: 1.75mm PLA

Analysis software: Matlab, Desmos

2.2 Engine

All data are based on Toyota 4A engine in American market[2].

Capacity: 1587cc

Maximum Power: 112hp at 6600rpm

Maximum Torque: 131Nm at 4800rpm

Valve degree: 50 degrees

Bore: 81mm (3.19in)

Stroke: 77mm (3.03in)

Crack pin: 42mm

I-beam connecting rod:

Center to center length: 122mm

Big end bore diameter: 44.98mm

Big end width: 21.82mm

Small end bore diameter: 19.99mm

Small end width: 21.82mm

Chapter 3

Tensile Testing

PLA (polylactic acid) is a popular material in 3D printing due to its properties. PLA is derived from renewable resources like sugarcane, making it an environmentally friendly and biodegradable option compared to petroleum-based plastics. Also, PLA is easy for printing. PLA exhibits good printability, with minimal warping, controlled shrinkage, and low tendency to clog nozzles, making it suitable for either beginners or experienced user.

PLA has moderate strength compared to other 3D printing materials. While it is suitable for many applications, particularly for prototypes, models, and non-functional parts, it is not the strongest material available for 3D printing. We will be looking for the strength of the model we print and the highest theoretical strength that PLA could have. The property of the material we are looking for is Young's modulus. Higher Young's modulus usually means higher strength. In order to get the Young's modulus of the printing material, I conducted tensile testing on the standard dogbone specimens using Instron machine. Tensile testing is a fundamental type of mechanical testing performed by engineers and materials scientists in manufacturing and research facilities all over the world. A tensile test (or tension test) applies force to a material specimen in order to measure the material's response to tensile (or pulling) stress. This type of testing provides insight into the mechanical properties of a material and enables product designers to make informed decisions about when, where, and how to use a given material.[3] From the machine,

the Young's modulus and yield stress will be given.

3.1 Dogbond Specimen

The dogbone specimen is the standard model for tensile testing[4]. With printing and testing the specimens printed in different angle, we can compare the result and Young's modulus to get the most ideal printing setting for achieving largest material strength.

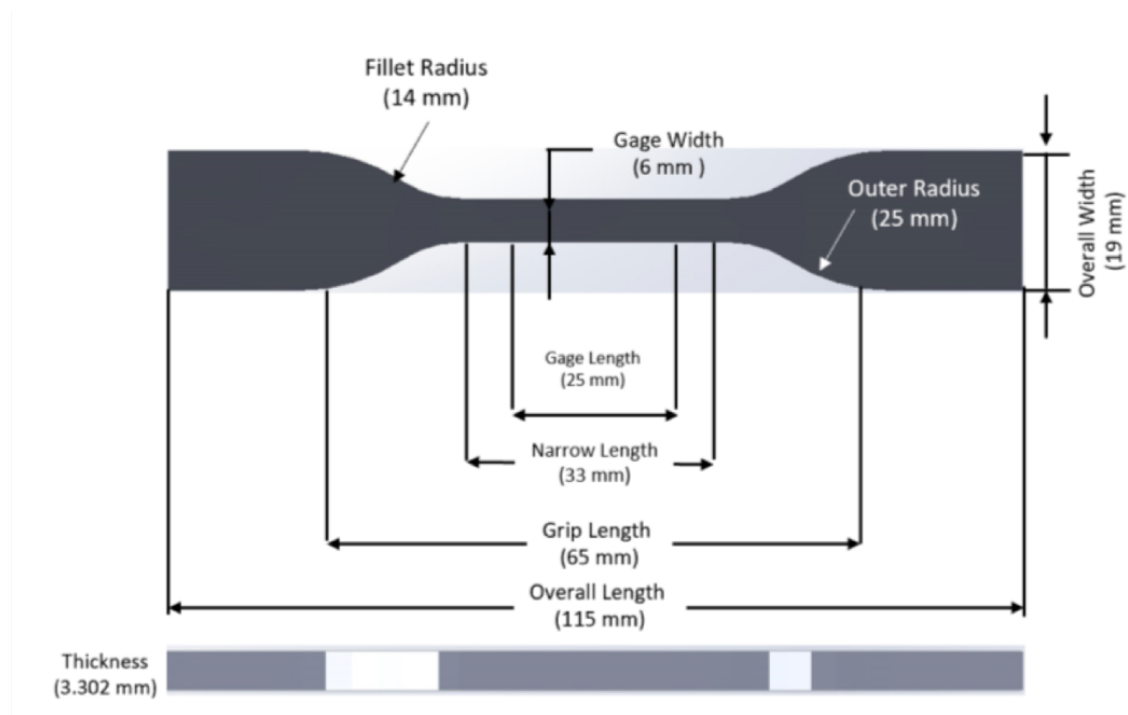


Figure 3.1: Standard dogbone specimens dimensions.

3.2 Result from Instron Tensile Machine Experimentation

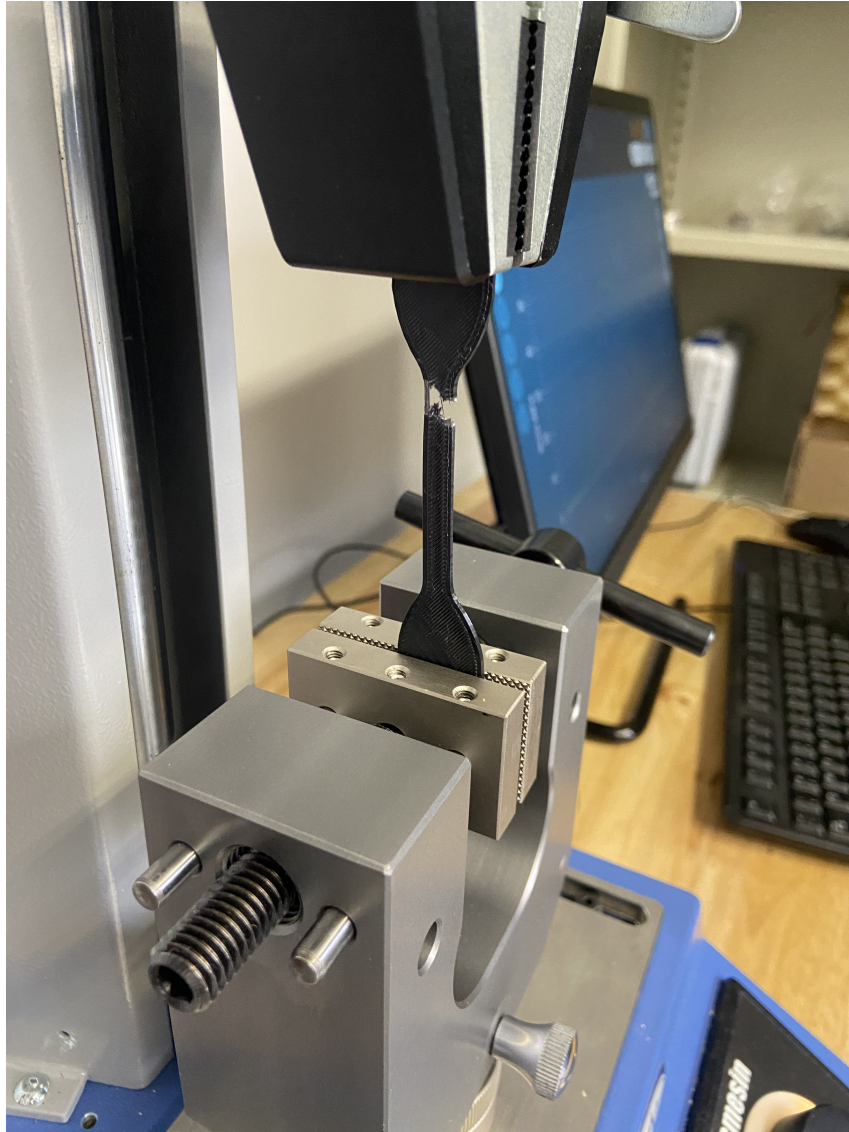


Figure 3.2: Tensile testing by using Instron machine.

The following graphs are the Stress-Strain graph generated by the Instron machine. The slope of the line at any instant point is Young's modulus. With the help of the machine, we can know the average Young's modulus of each trial easily.

The little triangle on the 0 printing degree and 50% infill rate rate graph represents how the Young's modulus is calculated, which is the stress change divided by strain change.

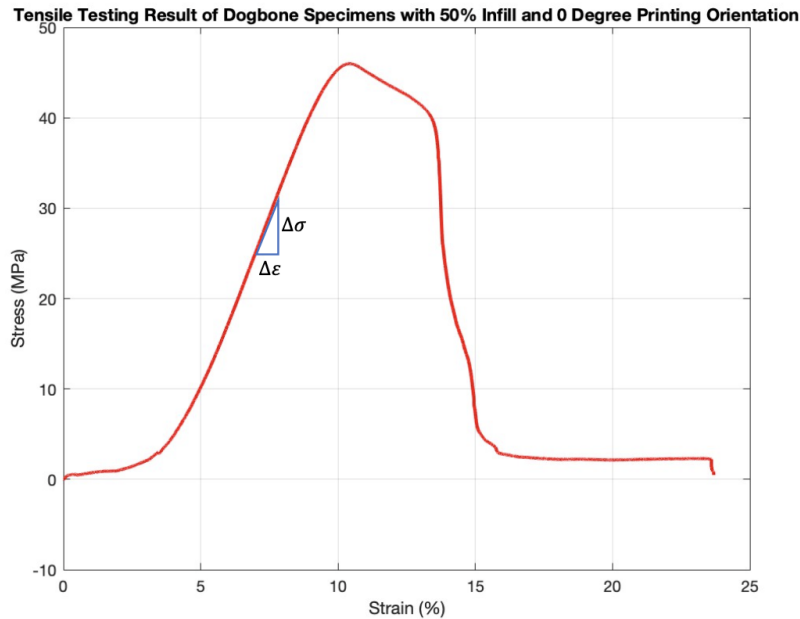


Figure 3.3: Tensile testing result of dogbone specimen printed in 0 degree and 50% infill rate.

The following table is result from the tensile testing. Among all these trials, the printing orientation in 0 degree and 50% infill rate is the printing setting for engine model. The three trials of 100% infill rate and 0, 45, 90 printing angle is used to test the strength of the printing material, which is PLA in this project[5]. As we can observe, when the infill rates are the same, the printing orientations determine the strength. When the printing angle is 90 degree, the Young's modulus is 557.829MPa, which is significantly smaller than specimens printed in 0 degree and almost only half of that in 45 degree printing orientation. At the same time, the largest yield stress also occurs in 45 printing orientation specimen, which is 53.09MPa. Meanwhile, we are expecting the density of the specimen with 50% infill

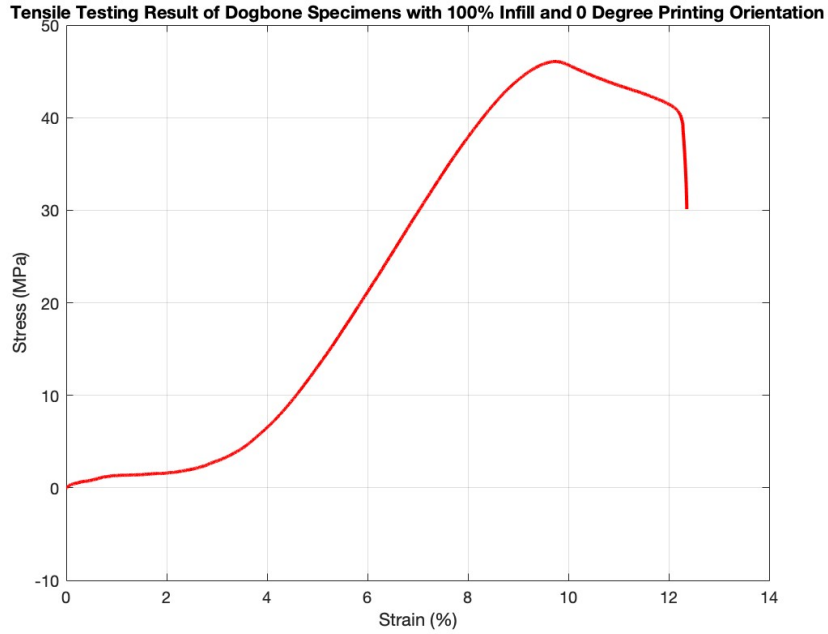


Figure 3.4: Tensile testing result of dogbone specimen printed in 0 degree and 100% infill rate.

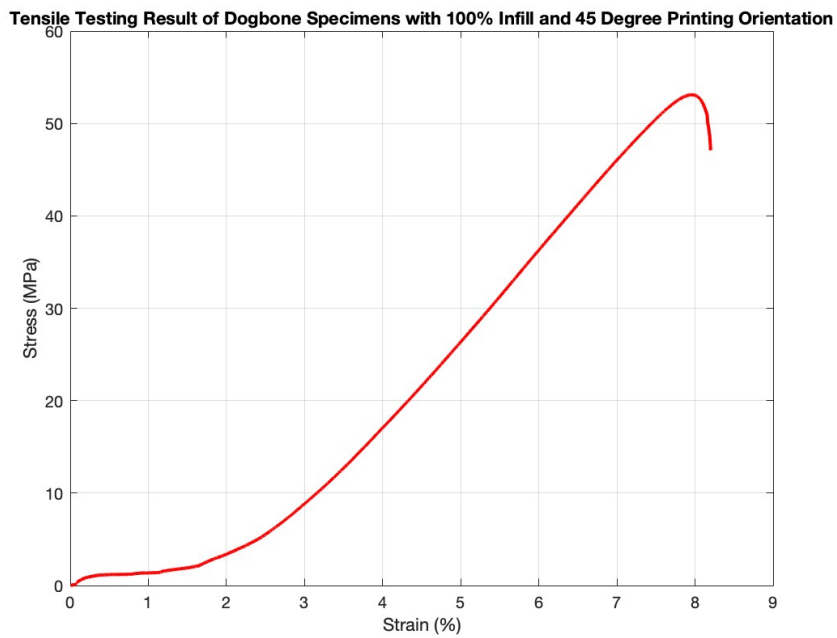


Figure 3.5: Tensile testing result of dogbone specimen printed in 45 degree and 100% infill rate.

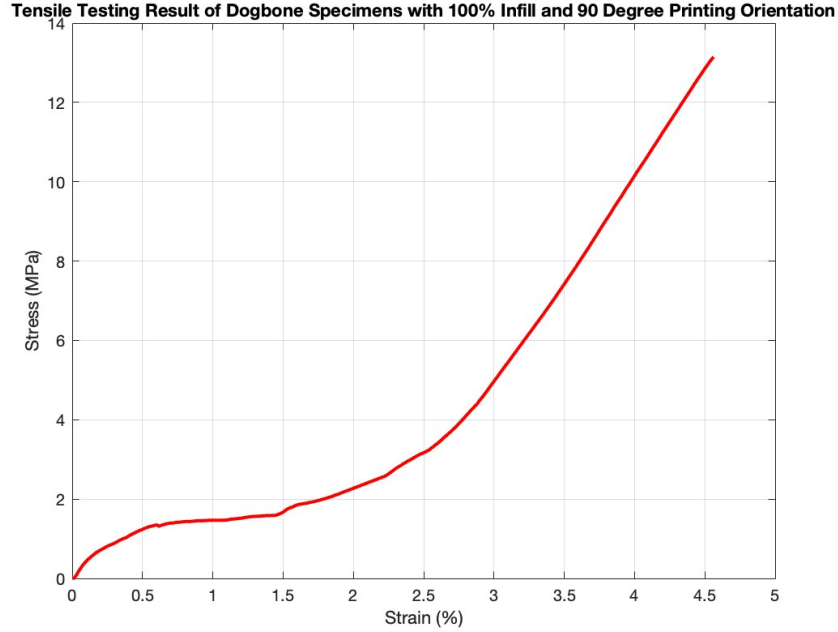


Figure 3.6: Tensile testing result of dogbone specimen printed in 90 degree and 100% infill rate.

rate is half of that of 100% infill rate because the volume is the same but the mass is half theoretically. However as we notice, the density is not half. The reason of this is because the specimens are very thin, most volume of the specimens is made up of surface. Therefore, the density of 50% infill rate specimens is larger than we expected.

Table 3.3: Results from the tensile testing.

Printing orientation (Degree)	Infill Rate (%)	Density (g/mm ³)	Young's Modulus (MPa)	Yield Stress (MPa)
0	50	8.29E-04	809.965	45.99
0	100	1.02E-03	874.637	46.07
45	100	1.02E-03	1014.319	53.09
90	100	1.02E-03	557.829	13.15

From the above table 3.7 and graphs, we can make a brief conclusion that the most ideal printing angle for getting largest strength of the printing material is 45 degree under the condition of same infill rate. In future application, when Young's

modulus is needed for calculation, instead of a very wide range, we could use the specific numerical results from this experimental research for more accurate results.

Chapter 4

Kinematic Analysis

This chapter will talk about the kinematic part of the Toyota 4A engine including the displacements, linear and angular velocities, along with linear and angular accelerations of different parts. There are two parts in this chapter, which are hand calculation and solidwork simulation. With calculating these variables by hand and comparing them with the results from 3D modeling software and textbook[6], we could verify the formula, and most importantly, have a better understanding of the principal of the internal combustion engine. All the calculation will be based on the actual size of the engine2.2.

4.1 Diagram

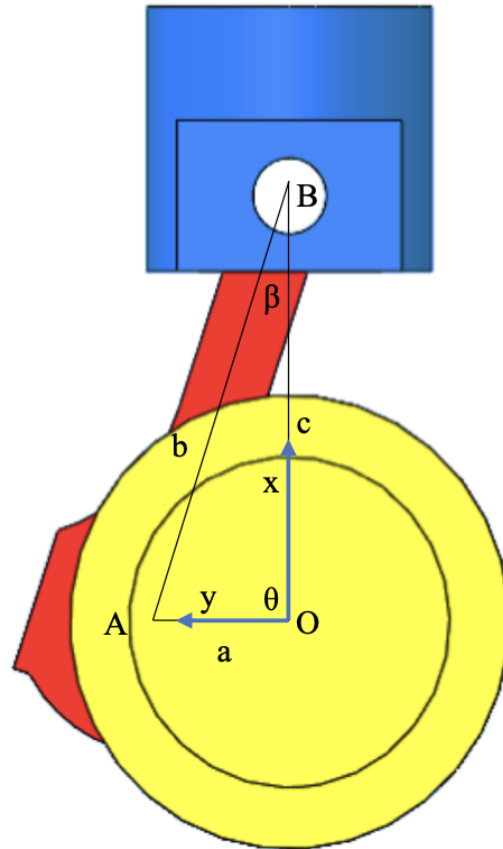


Figure 4.1: Diagram that represents the piston (blue), connecting rod (red), and crankshaft(yellow).

4.2 Hand Calculation

Let's define the spinning radius of the crankshaft as a ; the length of the connecting rod as b ; and the distance between piston and crankshaft as c 4.1. By using vector loop method, we could get an expression of the moving distance of piston as follows:

1 $\vec{OA} - \vec{AB} - \vec{OB} = 0$

2 $\beta = \sin^{-1} \frac{a \sin \theta}{b}$

3 **Displacement:**

4 $a(\cos \theta \hat{i} + \sin \theta \hat{j}) - b(\cos \beta \hat{i} + \sin \beta \hat{j}) - c\hat{i} = 0$, where \hat{i} and \hat{j} represents unit in x-
5 direction and y-direction respectively.

6 **In x-direction:**

7 $a \cos \theta - b \cos \beta - c = 0$

8 **In y-direction:**

9 $a \sin \theta - b \sin \beta = 0$

By taking derivatives on each term, we could generate the expression for both linear velocity and angular velocity as follows:

10 **Velocity:**

11 $a\dot{\theta}(-\sin \theta \hat{i} + \cos \theta \hat{j}) + b\dot{\beta}(\sin \beta \hat{i} + \cos \beta \hat{j}) - c\dot{\hat{i}} = 0$, where $\dot{\theta}$ and $\dot{\beta}$ represents the
12 derivative of displacement of angle θ and β . Therefore, we can rewrite the above
13 expression into:

14 $a\omega_A(-\sin \theta \hat{i} + \cos \theta \hat{j}) + b\omega_B(\sin \beta \hat{i} + \cos \beta \hat{j}) - v_B\hat{i} = 0$

15 **In x-direction:**

16 $-a\omega_A \sin \theta + b \omega_B \sin \beta - v_B = 0$

17 **In y-direction:**

18 $-a\omega_A \cos \theta + b\omega_B \cos \beta = 0$

By taking derivatives on each term again, we could generate the expression for both linear acceleration and angular acceleration as follows:

19 **Acceleration:**

$$20 \quad a[\dot{\omega}_A(-\sin \theta \hat{i} + \cos \theta \hat{j}) - \omega_A^2(\cos \theta \hat{i} + \sin \theta \hat{j})] - b[\dot{\omega}_B(\sin \beta \hat{i} - \cos \beta \hat{j})$$

$$21 \quad \quad - \omega_B^2(-\cos \beta \hat{i} + \sin \beta \hat{j})] - \ddot{c} \hat{i} = 0$$

22 where $\dot{\omega}_A$ and $\dot{\omega}_B$ represents the derivative of velocity of angle ω_A and ω_B . Therefore,
23 we can rewrite the above expression into:

$$24 \quad a[\alpha_A(-\sin \theta \hat{i} + \cos \theta \hat{j}) - \omega_A^2(\cos \theta \hat{i} + \sin \theta \hat{j})] + b[\alpha_B(\sin \beta \hat{i} + \cos \beta \hat{j})$$

$$25 \quad \quad - \omega_B^2(-\cos \beta \hat{i} + \sin \beta \hat{j})] - a_B \hat{i} = 0$$

26 **In x-direction:**

$$27 \quad -a\alpha_A \sin \theta - a\omega_A^2 \cos \theta + b\alpha_B \sin \beta - b\omega_B^2 \cos \beta - a_B = 0$$

28 **In y-direction:**

$$29 \quad a\alpha_A \cos \theta - a\omega_A^2 \sin \theta + b\alpha_B \cos \beta + b\omega_B^2 \sin \beta = 0$$

The result of all the kinematic variables are as follows:

30 **Results:**

$$31 \quad c = a \cos \theta - b \cos(\sin^{-1} \frac{a \sin \theta}{b}) \quad (\text{Piston displacement})$$

$$32 \quad v_b = -a\omega_A \sin \theta + b \omega_B \sin \beta \quad (\text{Piston velocity})$$

$$33 \quad \omega_B = \frac{a \cos \theta}{b \cos \beta} \omega_A \quad (\text{Angular velocity, where } \omega_A \text{ is the angular velocity of the crankshaft})$$

$$34 \quad a_B = -a\alpha_A \sin \theta - a\omega_A^2 \cos \theta + b\alpha_B \sin \beta - b\omega_B^2 \cos \beta \quad (\text{Piston linear acceleration})$$

$$35 \quad \alpha_B = \frac{a\omega_A^2 \sin \theta + b\omega_A^2 \sin \beta}{b \cos \beta} \quad (\text{Piston angular acceleration})$$

4.3 Solidwork Simulation

In this section, I will be graphing the expressions from the previous 4.2 section to verify. There will be results only for one cylinder instead for four cylinders because the result for the first cylinder and the fourth cylinder are the same and the result for the middle two cylinders are flipped along y-axis with the same magnitude.

4.3.1 Piston Displacement

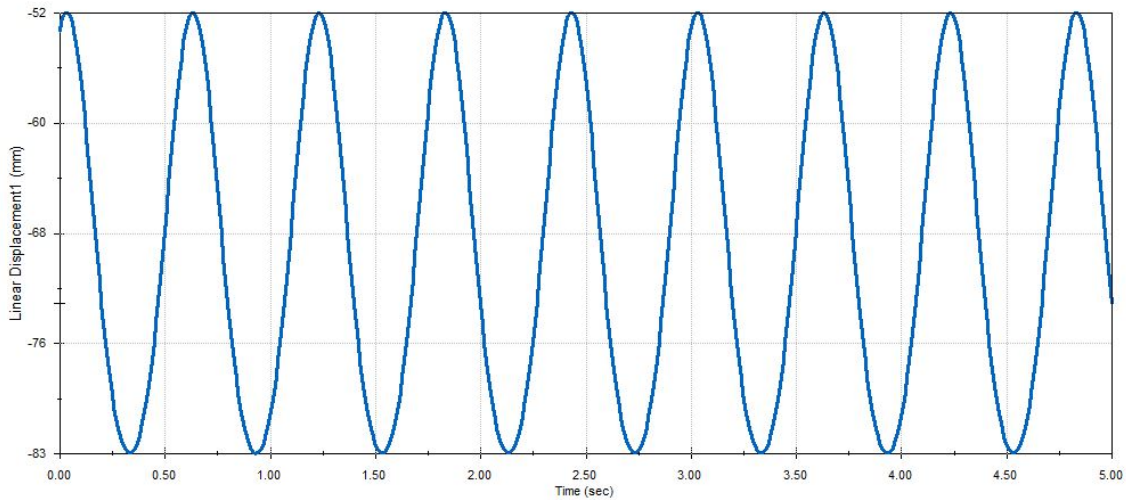


Figure 4.2: Piston displacement graph generated from Solidworks motion analysis.

4.3.2 Linear Velocity of Piston

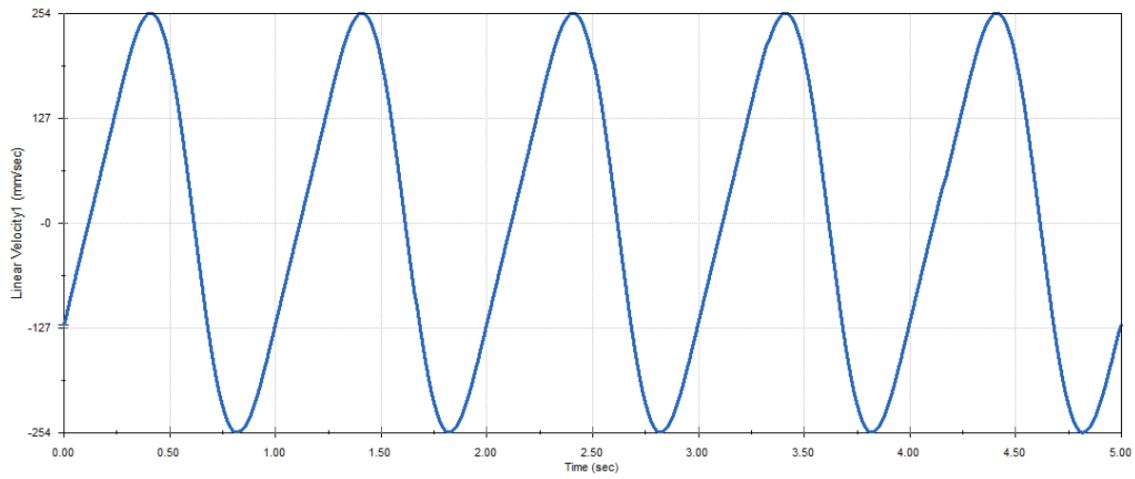


Figure 4.3: Motion analysis of linear velocity of piston using Solidworks

4.3.3 Angular Velocity of Connecting Rod

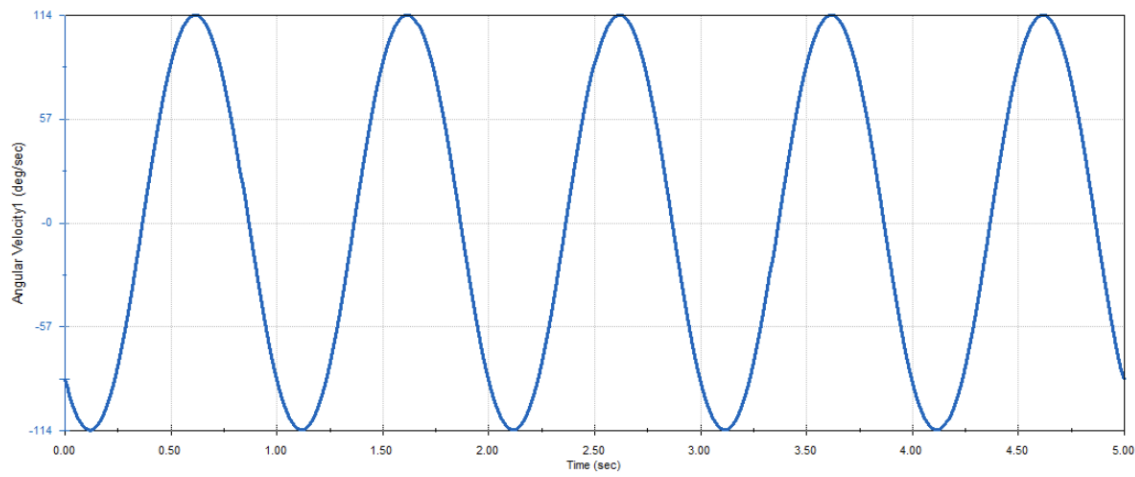


Figure 4.4: Motion analysis of angular velocity of connecting rod using Solidworks.

4.3.4 Angular Acceleration

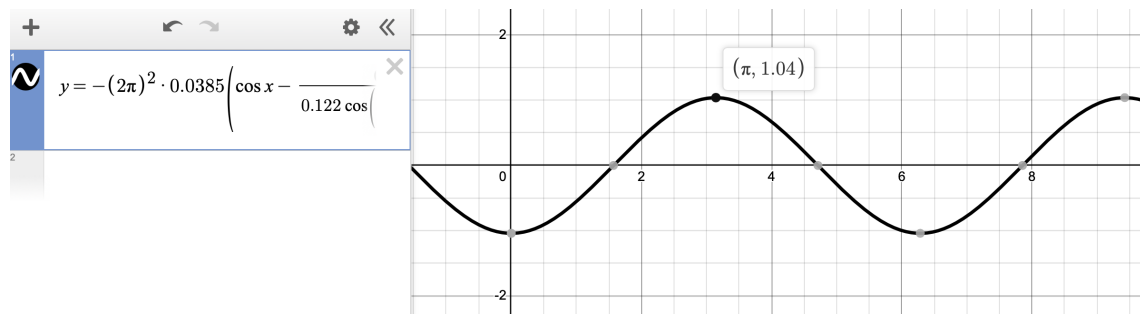


Figure 4.5: The hand calculated angular acceleration of the connecting rod graphed using Desmos.

Chapter 5

Dynamic Analysis

In this chapter, we will use the results of the kinematic analysis 4.2 to do the dynamic analysis to get to know the motion of the engine better. We will also do the hand calculation and verify it with the software simulation and with the textbook[6].

5.1 Diagram

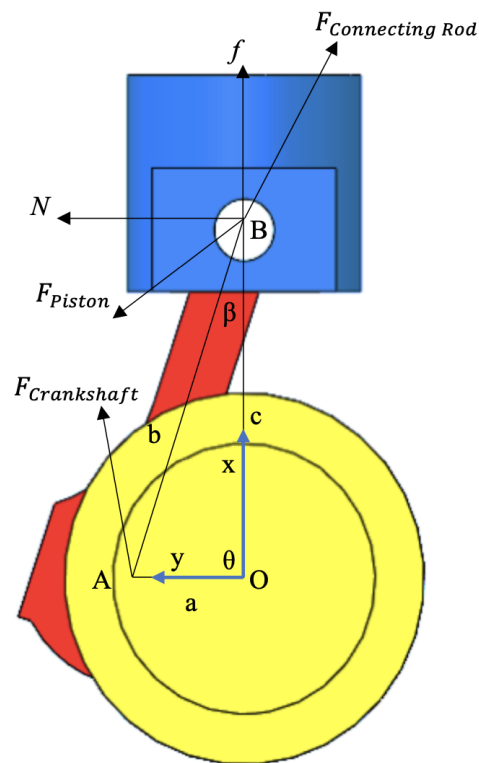


Figure 5.1: Free body diagram of the crankshaft system.

5.2 Hand Calculation

By solving sum of force and sum of momentum, we could easily get the expression for every force as follows:

Force on Piston

$$\sum F_x = F_{CR,x} - N = 0$$

$$\sum F_y = F_{CR,y} - F_f - F_G = m_{piston} a_{piston}$$

Moment on Piston

There is no arms for every force because the forces go through the center of mass of the piston.

Therefore,

$$\sum M_{piston} = 0$$

Force on Connecting Rod

$$\sum F_x = F_{C,x} - F_{CR,x} = m_{CR} a_{CR,x}$$

$$\sum F_y = F_{C,y} - F_G - F_{CR,y} = m_{CR} a_{CR,y}$$

Moment on point B

$$\sum M_B = F_{CR,x} \cdot \frac{L}{2} \cdot \sin \theta - F_{CR,y} \cdot \frac{L}{2} \cdot \cos \theta = I \alpha$$

Result

$$F_{CR,x} = \frac{I \alpha + m_{piston} a_{piston} \cdot L \cdot \cos \theta}{L \cdot \sin \theta}$$

$$F_{CR,y} = m_{piston} a_{piston}$$

$$F_{C,x} = m_C \cdot a \cdot \sin \beta$$

$$F_{C,y} = m_C \cdot a \cdot \cos \beta + m_{piston} a_{piston}$$

5.3 Solidworks Simulation

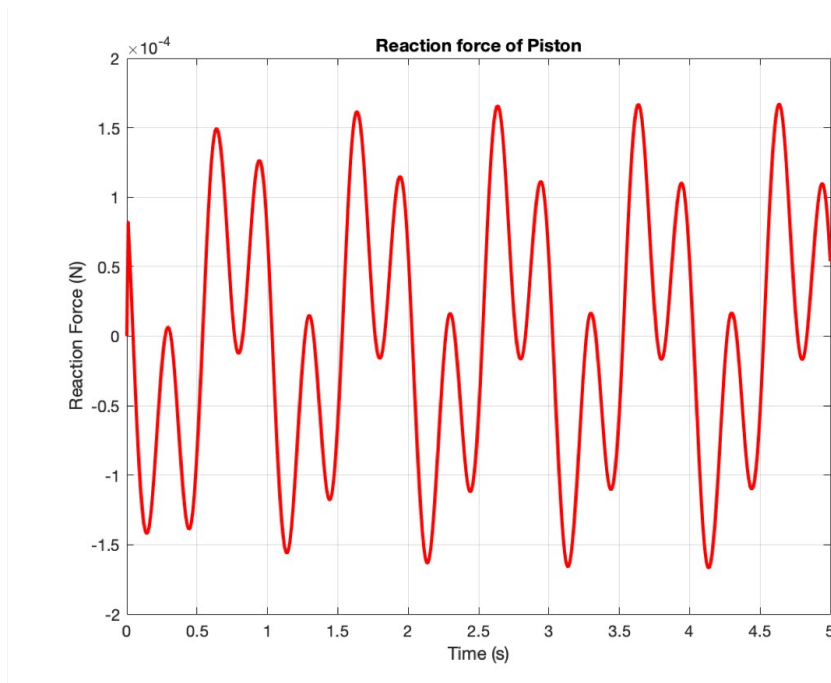


Figure 5.2: Reaction force between piston and cylinder body generated by matlab.

The graph looks not in regular sinusoidal or any trigonometry function because there is friction affected the reaction force. Also, normal force exist, which also affect the magnitude of the reaction force of piston. With the effects of normal force and friction force, the magnitude still matches with the hand calculation. In the real engine, engineers always try to minimize the friction between the piston and the cylinder body so that the efficiency of the engine will be maximized.

Chapter 6

Conclusion

In conclusion, 3D printing an internal combustion engine (ICE) model with PLA offers several advantages, such as cost-effectiveness, rapid prototyping, and design flexibility. This approach is particularly suitable for educational purposes, where the focus is primarily on understanding the motion and functionality of the engine components.

However, it is necessary to consider the limitations of PLA material, including its lower mechanical strength and heat resistance compared to traditional engine materials. These limitations restrict the use of PLA 3D printed ICE models in functional applications or high-stress environments. Additionally, attention should be given to selecting the appropriate material, ensuring safety, and addressing engineering ethics when developing and using PLA 3D printed engine models.

Meanwhile, tensile testing is an important method in engineering. It provides necessary data on the properties of materials. By putting a material to a controlled tension until it breaks, tensile testing helps determine properties such as Young's modulus, elongation, and yield strength. These properties play an important role in selecting material, manufacturing, and theoretical analysis.

In summary, while PLA 3D printed ICE models provide possibilities for prototyping and education, their applications are limited by the material's properties. By doing the same test on different materials, we could decide the most desired material to meet our needs.

Chapter 7

Impact

Engineering ethics involves adhering to ethical principles, professional standards, and practices while designing, manufacturing, and testing products[7]. In the context of a PLA 3D printed engine, several ethical considerations should be addressed:

7.1 Safety

Ensuring that the 3D printed engine is safe to use, handle, and operate is crucial. Since PLA has a lower heat resistance and strength compared to traditional engine materials, it is essential to inform users of the limitations and potential risks associated with using a PLA 3D printed engine model.

7.2 Environment

PLA is a biodegradable material, which is a positive step toward reducing environmental impact. However, engineers should also consider the entire lifecycle of the 3D printed engine, including energy consumption during manufacturing and disposal or recycling options.

7.3 Education

Engineers should maintain and develop their knowledge and skills in 3D printing and engine design to ensure they provide accurate and up-to-date information.

7.4 Economic

3D printing with PLA can be an economical option for creating prototypes and educational models. The lower cost of PLA and the accessibility of FDM 3D printers make it a cost-effective choice for initial development stages, reducing the need for expensive traditional manufacturing processes.

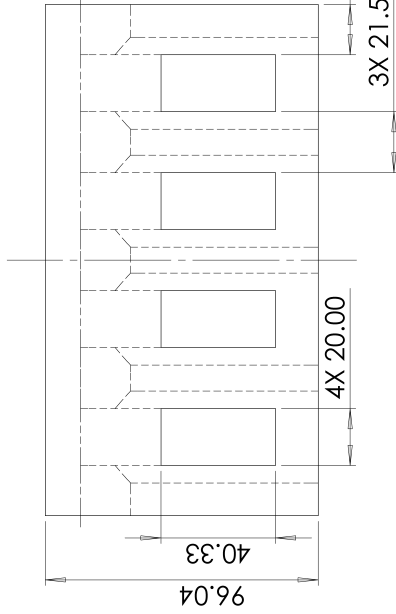
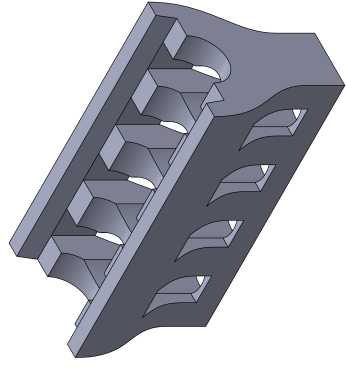
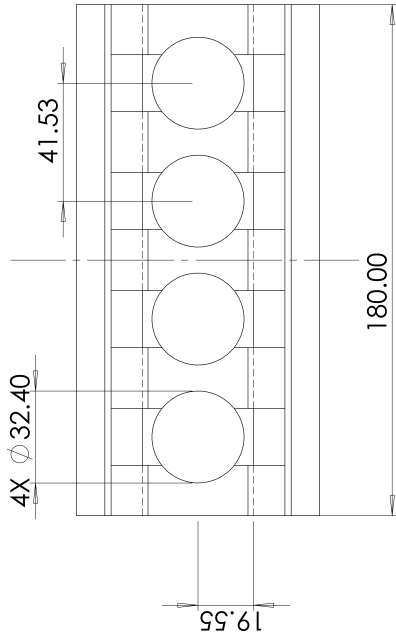
Appendices

Appendix A

CAD Drawing

2

1



Dimensions of the curve:

Parameters

1	<	>
-42.78796704	<	>
96.04	<	>
0.00	<	>
114.85506625	<	>
-90.00°	<	>

Tangent driving
 Proportional

Reset This Handle
Reset All Handles
Relax Spine

B

A

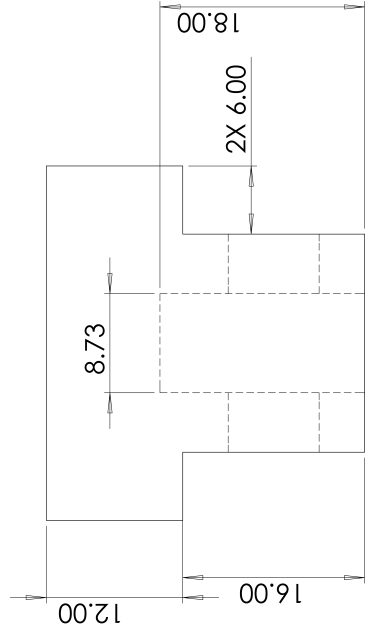
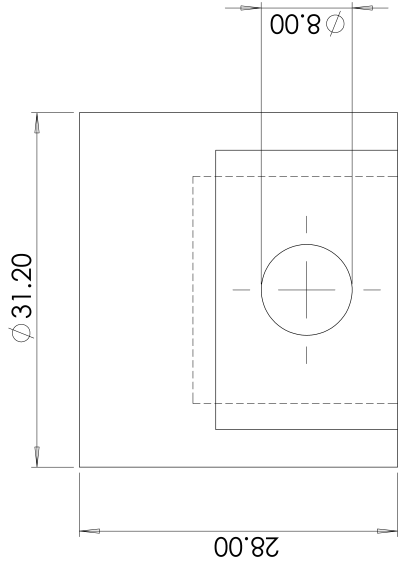
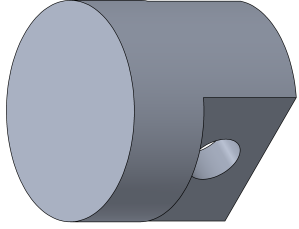
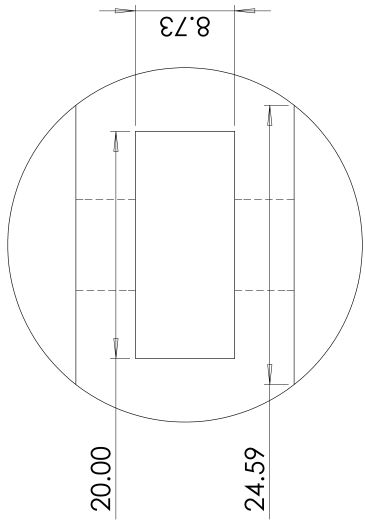
Mechanical Engineering Department Worcester Polytechnic Institute	UNLESS OTHERWISE SPECIFIED DIMENSIONS ARE IN MILLIMETERS. TOLERANCES ARE .XX ± .005 .XXX ± .001 ANGLES ± 1. DIMENSIONING AND TOLERANCE IN ACCORDANCE WITH ASME.Y14.5-2018	MATL: PLA	TITLE: Engine Body
	DRAWN BY: Qianchen Zeng	DATE: Mar.28, 2023	SCALE: 1:2 DWG. NO. 1001

B

A

1

2



B

B

A

A

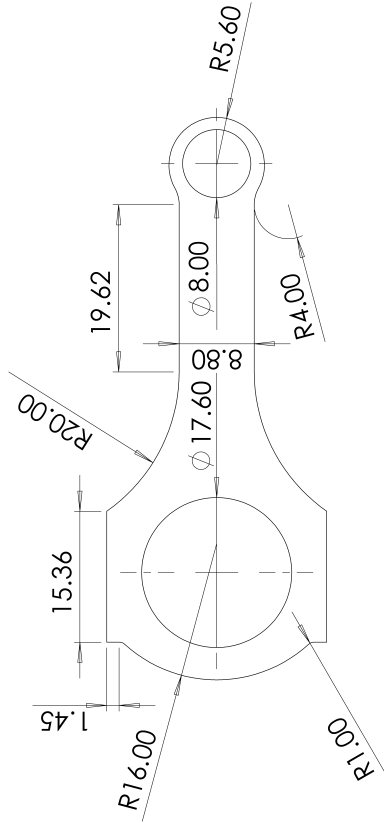
Mechanical Engineering Department Worcester Polytechnic Institute	UNLESS OTHERWISE SPECIFIED DIMENSIONS ARE IN MILLIMETERS. TOLERANCES ARE .XX ± .005 .XXX ± .001 ANGLES ± 1°. DIMENSIONING AND TOLERANCE IN ACCORDANCE WITH ASME.Y14.5-2018		MATL: PLA	TITLE: Piston
	DRAWN BY: Qianchen Zeng		DATE: Apr. 6, 2023	DWG. NO. 1002
	SCALE: 2:1		1	

2

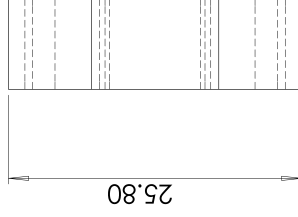
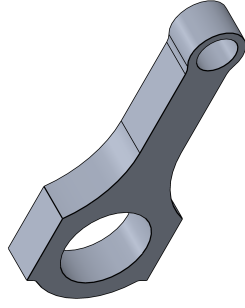
1

1

2



B



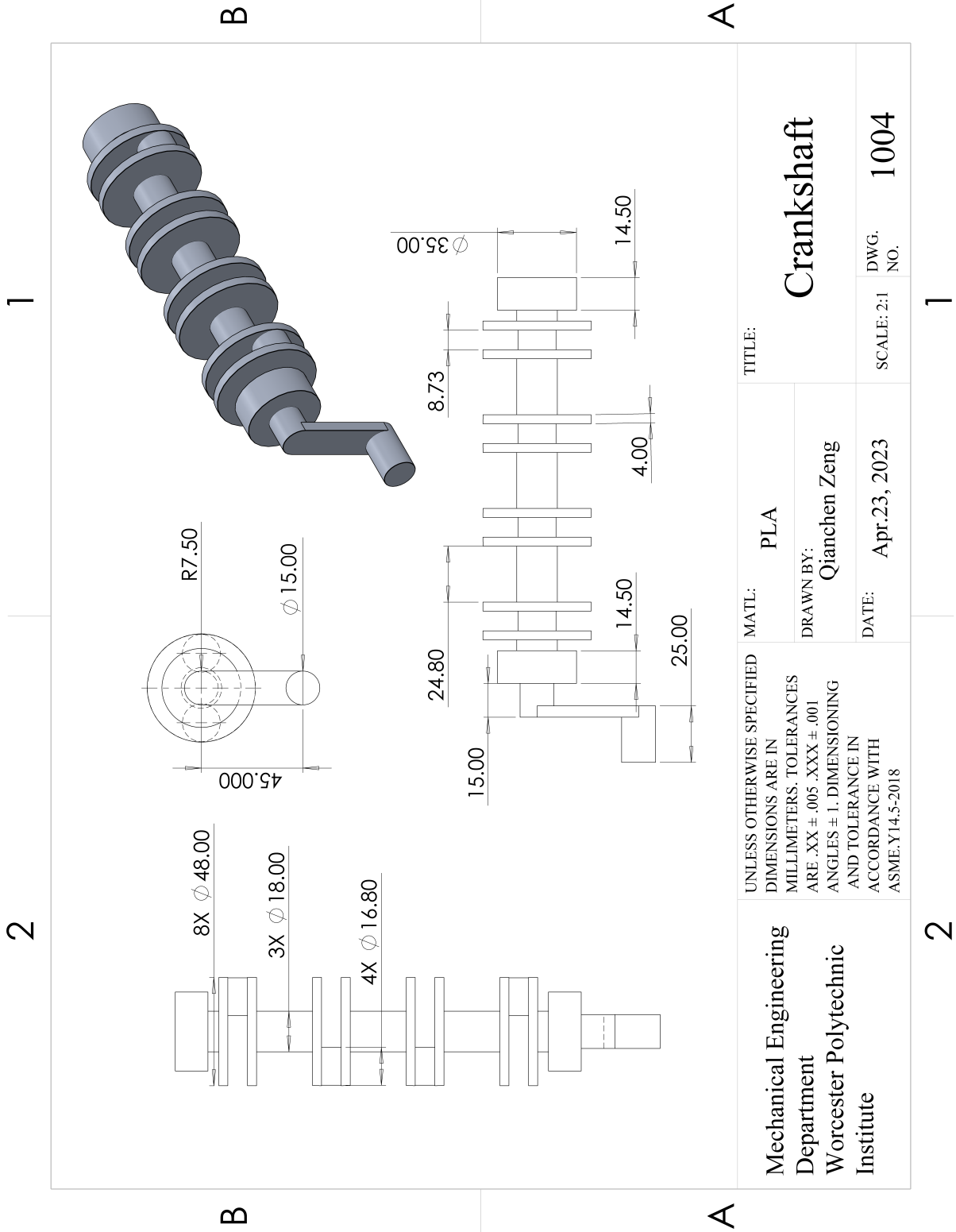
A

A

Mechanical Engineering Department Worcester Polytechnic Institute	UNLESS OTHERWISE SPECIFIED DIMENSIONS ARE IN MILLIMETERS. TOLERANCES ARE .XX ± .005 .XXX ± .001 ANGLES ± 1. DIMENSIONING AND TOLERANCE IN ACCORDANCE WITH ASME.Y14.5-2018	MATL: PLA DRAWN BY: Qianchen Zeng DATE: Apr.23, 2023	TITLE: Connecting Rod SCALE: 1.5:1 DWG. NO. 1003
	Mechanical Engineering Department Worcester Polytechnic Institute		

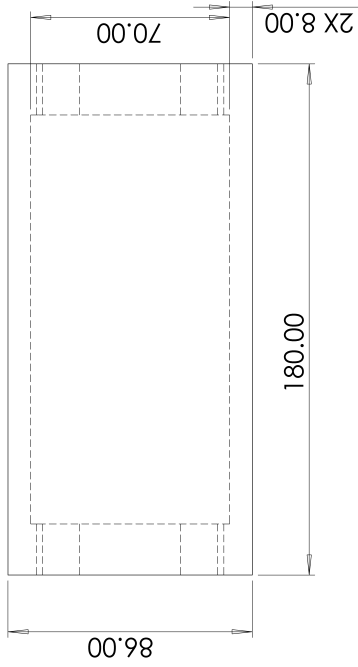
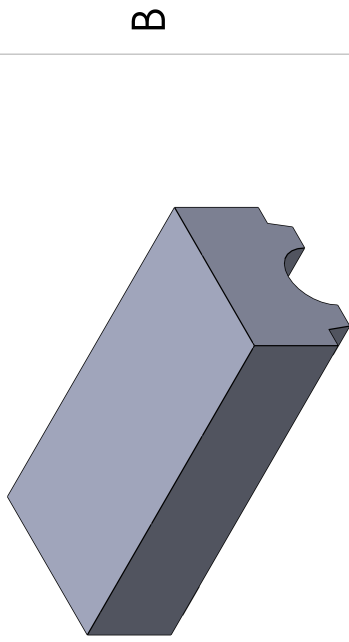
2

1



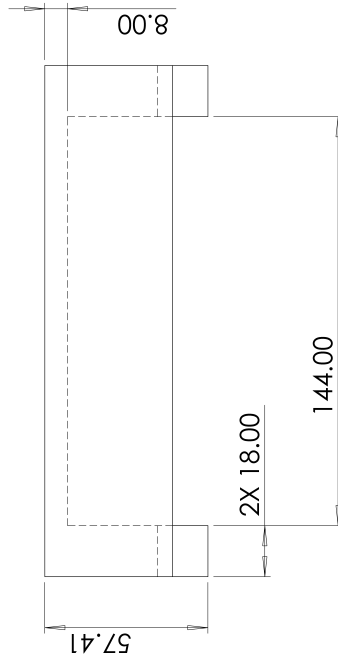
2

1



B

B



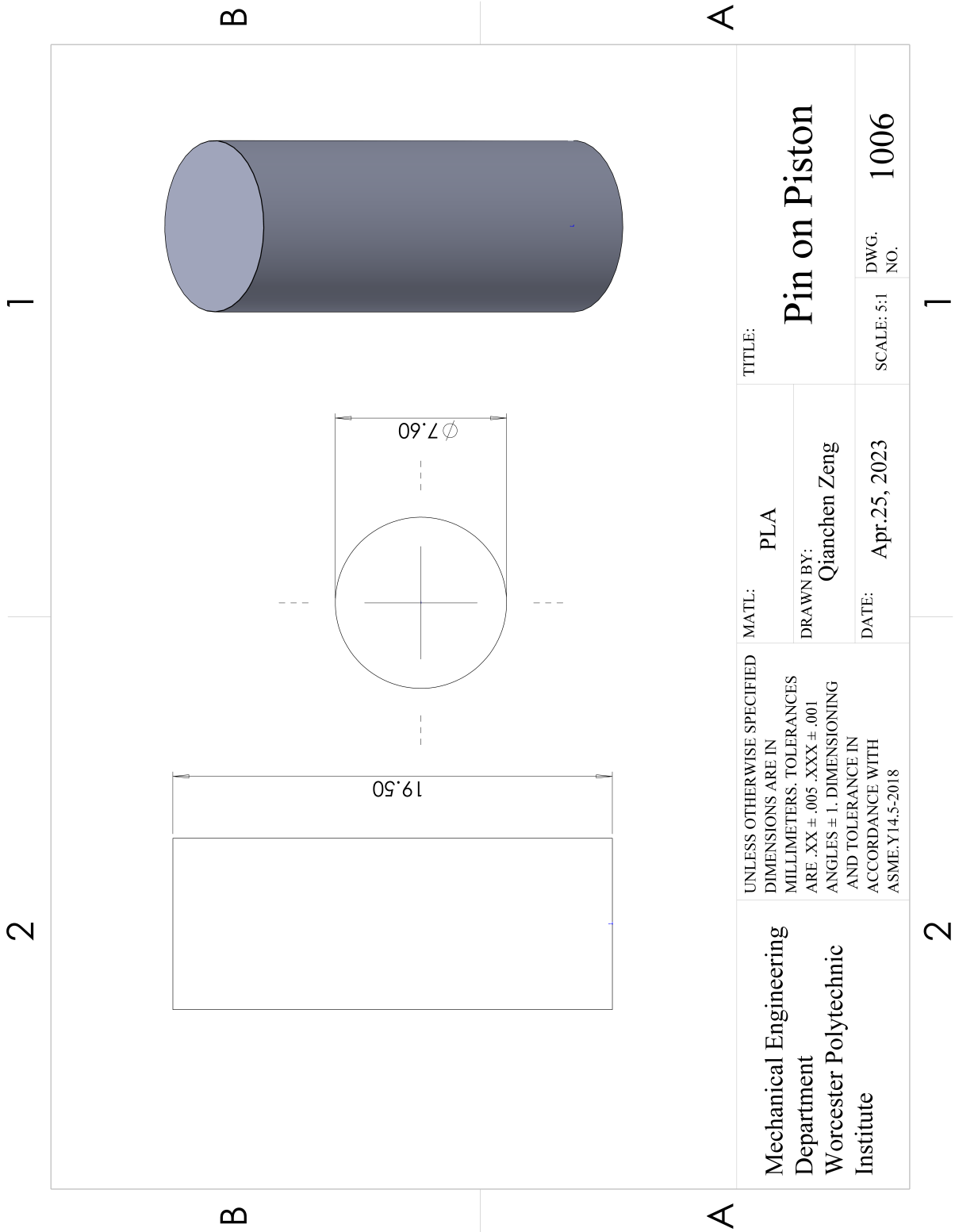
A

A

Mechanical Engineering Department Worcester Polytechnic Institute	UNLESS OTHERWISE SPECIFIED DIMENSIONS ARE IN MILLIMETERS. TOLERANCES ARE .XX ± .005 .XXX ± .001 ANGLES ± 1°. DIMENSIONING AND TOLERANCE IN ACCORDANCE WITH ASME.Y14.5-2018		MATL: PLA	TITLE: Engine Body Cover
	DRAWN BY: Qianchen Zeng	DATE: Apr.24, 2023	SCALE: 1:2	DWG. NO. 1005

2

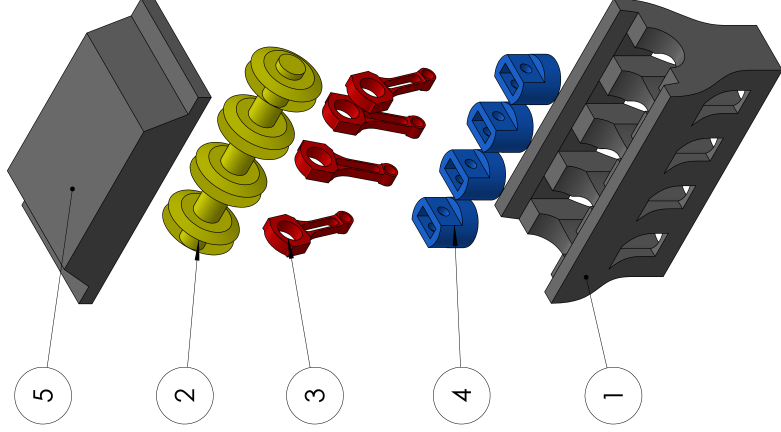
1



2

1

ITEM NO.	PART	QTY.
1	Lower Cylinder Body	1
2	Crankshaft2	1
3	Connecting Rod	4
4	Piston	4
5	Lower Cylinder Body Cover	1



B

B

A

A

Mechanical Engineering Department Worcester Polytechnic Institute	MATL: PLA	TITLE: Engine Assembly
	DRAWN BY: Qianchen Zeng	SCALE: 1:3.5
UNLESS OTHERWISE SPECIFIED DIMENSIONS ARE IN MILLIMETERS. TOLERANCES ARE .XX ± .005 .XXX ± .001 ANGLES ± 1°. DIMENSIONING AND TOLERANCE IN ACCORDANCE WITH ASME.Y14.5-2018		DATE: Mar. 29, 2023

2

1

Bibliography

- [1] Zachary Killoy Eric Brigman, Chris Destefano. Slider – crank mechanism for demonstration and experimentation. 2013.
- [2] MyMotorList.com. Engine toyota 4a-gze, 2023.
- [3] INSTRON.com. Tensile testing.
- [4] Shivraj Narayan Yeole. Tensile testing and evaluation of 3d printed plaspecimens as per astm d638 type-iv standard. February 2018.
- [5] BioPak. What is pla?, 2020.
- [6] Robert L. Norton. *Design of Machinery*. McGraw Hill, sixth edition edition, 2019.
- [7] ASME. Code of ethics of engineers, 2012.